Nuclear Instruments and Methods 177 (1980) 239–246

FIRST RESULTS OF THE WORK WITH A SUPERCONDUCTING "SNAKE" AT THE VEPP-3 STORAGE RING

A.S. ARTAMONOV, L.M. BARKOV, V.B. BARYSHEV, N.S. BASHTOVOY, N.A. VINOKUROV, E.S. GLUSKIN, G.A. KORNIUKHIN, V.A. KOCHUBEI, G.N. KULIPANOV, N.A. MEZENTSEV, V.F. PINDIURIN, A.N. SKRINSKY and V.M. KHOREV
Institute of Nuclear Physics, 630090, Novosibirsk, USSR

1. Introduction

In 1977 a project to install a superconducting "snake" with maximum field of 35 kG on the storage ring VEPP-3 was reported [1,2]. The synchrotron radiation beam brightness was planned to be a maximum in the range $\lambda \sim 1.3$ Å for an electron energy of 2.2 GeV. The fabrication of a snake, a vacuum chamber necessary for installing this snake on the storage ring and also the correction magnets was completed by the end of 1978.

The first cycle of operation with a superconducting snake and an electron beam in the storage ring was carried out in April–June of 1979. Unfortunately, the high current supply for the correction magnets was not ready at that time, and for this reason the work was performed at an energy of 350 MeV (injection energy), using the power supply avalaible. The operation may be divided into three stages: (1) insertion of the electron beam into the narrow section of the snake vacuum chamber with the snake off; (2) compensation of the influence of the snake field on the stored beam; (3) a study of the spectral and angular characteristics of the undulator radiation from the snake at different values of the magnetic field. During the first trial runs a maximum field of about 36 kG was obtained in the snake both out of and also in the storage ring VEPP-3 without an electron beam.

The behavior of the beam was analysed for the case when the beam was inserted into the narrow section of the chamber with the help of correction magnets and when the field in the snake was switched on up to about 20 kG at an energy of 350 MeV. The results of the measurements of the angular and spectral characteristics of undulator radiation from the snake are given below.

2. The design of the superconducting snake and results of tests

The design of the snake is shown schematically in fig. 1. The unit (8) consists of 20 pairs of superconducting magnets which generate the alternating 35 kG field with a half-period of 4.5 cm. The magnet windings are made of partly stabilized NbTi cable of 0.7 mm diameter.

Liquid helium is supplied from a 100 l dewar [3]. The section of the storage ring vacuum chamber inside the snake is cooled with liquid nitrogen. The superconducting magnets (SCMs) of which the snake is composed, were tested in a special cryostat directly after their fabrication. We tested the SCMs blocks which contained from 4 to 20 SCMs arranged in the same way as in the snake. To detect quenches, the potential conductors from the SCMs connection points were used. All the SCMs were connected in series to the power supply; SCMs were indium-sealed over a 30 mm length.

In the event of a quench, the voltage jump on the "quenched" magnet occurs simultaneously with the associated appearance of the active resistance in its winding. By virtue of the inductive coupling, the voltage jump (but with opposite sign) takes place on the remaining SCMs as well. For detection of the first "quenched" magnets in the block, the multichannel threshold scheme was used the entrances of which were connected to individual SCMs, or a group of magnets. When one of the entrances is operated, the rest are blocked.

During the tests on the SCMs the training effect was clearly observed. The critical current after a sufficient number of quenches usually increased from 130 up to 220 A, which corresponds to the field of 36 kG, and then reached a plateau.

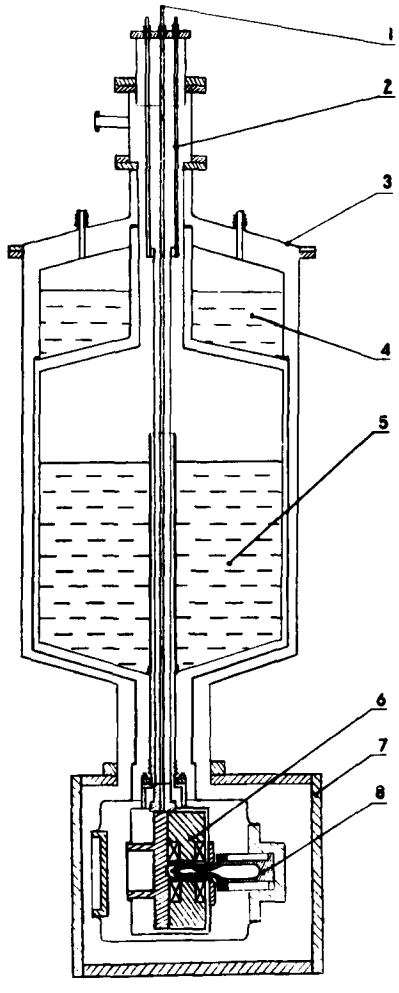

Fig. 1. A general view of the snake for the storage ring VEPP-3; 1 – liquid helium supply pipe, 2 – current leads, 3 – dewar, 4 – liquid nitrogen, 5 – liquid helium, 6 – superconducting magnets, 7 – vacuum container, 8 – storage ring vacuum chamber.

The number of quenches required in order to reach the plateau was approximately proportional to the general number of SCMs connected in series and was equal to 3–4 quenches per magnet.

The threshold showed that during the training process each of the SCMs is quenched occasionally, approximately the same number of times, except for the edge magnets where the number of quenches was 1.5 times higher.

In the complete block the number of windings in the edge magnets was decreased by 30%, that enabled us to partly compensate for the horizontal angle acquired by the beam at the snake exit and also to increase the SCM stability. Apparently, the training process can be explained by reference to the mechanical seal of the SCM winding in the direction of the forces acting on the current carrying windings. In this case, the interwinding filter (fiberglass tissue impregnated with epoxide compound) is a sufficiently dense, inelastic medium which is capable of "remembering" the training result. The training results are also conserved after the uniform heating of the SCM up to room temperature with subsequent cooling. As a rule, additional training with far fewer cycles is needed after the disassembly and reassembly of the magnetic system.

For preliminary tests the snake was assembled on the "bench". The maximum current supplied to the SCMs on the bench was 220 A, which corresponds to a field of 36 kG on the snake axis. Helium consumption in the field-off regime was 3.6 l/h. The measured shift of the SCMs with respect to the horizontal plane during cooling from room temperature to 4.2 K did not exceed 0.3 mm.

After the bench tests the snake was installed in the straight section of the VEPP-3 storage ring. The snake design made it possible to mount it around the VEPP-3 vacuum chamber without deterioration of the vacuum in the storage ring.

During the first switching-on of the snake, the SCM training was conducted once more. After five cycles the critical current in the SCM increased from 146 up to 190 A. The last figure corresponds to a field of $B_0 = 31$ kG on the snake axis. A further training of the SCM will be carried out during the forthcoming work on the snake. The measured helium consumption with the field on was ≤ 4 l/h.

3. Insertion of the electron beam into the snake with superconducting field off

Insertion of the "damped" electron beam into the snake vacuum chamber is performed by four special correction magnets of rectangular shape placed in the experimental straight section. In addition, a special magnetic straight-section structure was chosen to facilitate orbit distortion, arrangement of the snake and correction magnets. The structual alterations were such that, on the one hand, a straight section could be supplied with a unit transport matrix in both directions and, on the other hand, to make effective use of the lens magnetic fields in the case of orbit distortion.

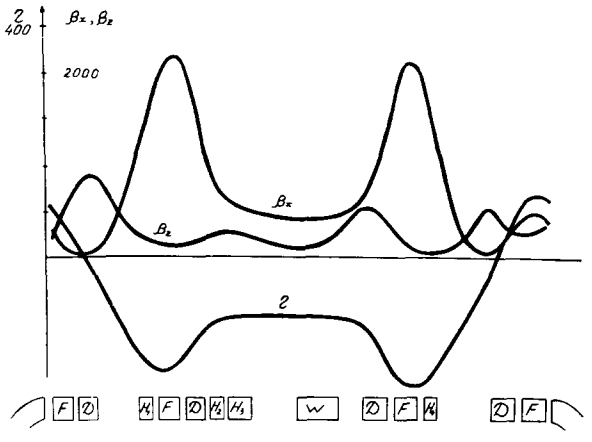

Fig. 2. Scheme for spacing the snake and correction magnets in the experimental straight section.

The scheme for spacing the snake and correction magnets in the experimental straight section is shown in fig. 2. Moreover, we can see the amplitude functions β_x and β_z, and the dispersion function η in this figure.

After the beam is "damped" to its stationary size and the beam energy is increased up to necessary value, a slow increase of the current in the correction magnets is carried out with a computer, this leads to a local orbit distortion and also to a beam shift up to 12 cm over the radius when the beam is inserted into the snake operating region.

The parameters of the correction magnets in the orbit distortion regime at an energy of 2 GeV are quoted in table 1.

One of the main difficulties which arises in case of the beam insertion into the vacuum chamber narrow section is to correct the orbit in the vertical direction inside the vacuum chamber of the snake.

This problem was solved with an accuracy of up to 1 mm with the help of two pick-up stations located in the experimental straight section and also by employing the transition matrices from the pick-up stations at the snake location.

A more precise vertical adjustment of the beam with respect to the vacuum chamber is carried out by visual observation of the synchrotron radiation beam from the snake operated with a weak field with the help of a telescope tube spaced at a distance of about 15 m from the snake.

In the event of orbital distortion, some effects must be taken into account.

(1) Appearance of the shift of betatron oscillation frequencies $\Delta\nu_x$ and $\Delta\nu_z$ as a result of the action of: (a) the edge focusing of the correction magnets which results in the vertical shift of the betatron oscillation frequency by the quantity $\Delta\nu_z \sim 0.02$, this shift being quadratic over a field in the magnets (in the radial direction the edge focusing is compensated by the curvature effect); (b) the nonlinear terms of the field expansion in the lenses wherein a large orbital distortion occurs (up to 3 cm) when the beam is inserted into the narrow section of the vacuum chamber (estimates based upon magnetic measurements of the lenses yield frequency shifts of $\Delta\nu_x$, $\Delta\nu_z \sim 10^{-2}$).

The correction of the frequencies is performed by the nearby lenses of the VEPP-3 magnetic structure, which have individual power supplies.

(2) When the beam is inserted into the snake, the orbit distortion at a constant frequency of revolution leads to a decreasing particle energy of

$$\Delta E/E = -(1/\alpha)(\Delta\Pi/\Pi) ,$$

where α is the delaying factor and Π the circumference of the storage ring. In the case of orbital distortion the energy change can lead to a change in the betatron oscillation frequencies if non-zero chromaticity occurs in the storage ring. Furthermore, the change in energy will occur with a change of the beam closed orbit by the amount

$$\Delta X = -(\eta/\alpha)(\Delta\Pi/\Pi) .$$

Table 1

	Magn. length (cm)	Magn. field H (kG)	Current in windings (kA)	Consump. power (kW)	Gap between poles (cm)	Oper. region over radius (cm)
H_1	21.8	7.66	0.868	3.7	4.5	3
H_2	38.4	17.38	1.61	19.8	3	9
H_3	65.43	−17.55	1.5	27.4	3	13
H_4	21.8	7.54	0.855	3.6	4.5	3

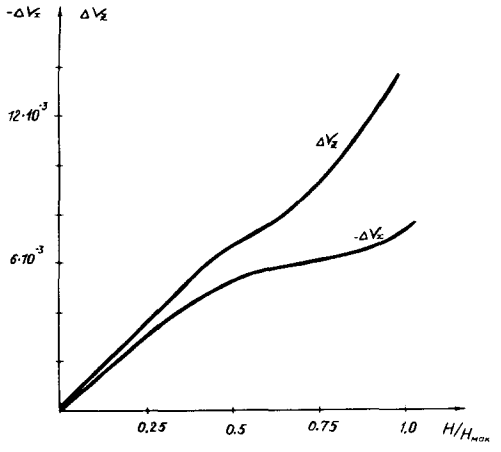

Fig. 3. Graphs of the experimentally measured $\Delta\nu_x$ and $\Delta\nu_z$.

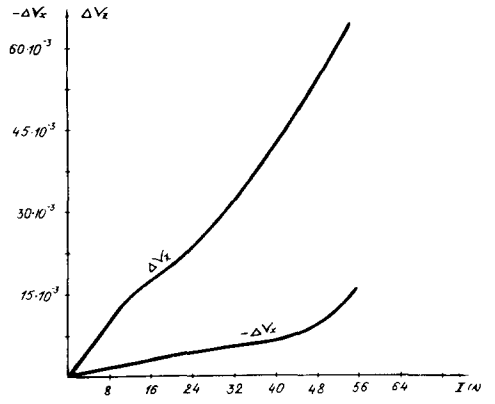

Fig. 4. Behavior of $\Delta\nu_x$ and $\Delta\nu_z$ versus the current in the snake.

This effect can be compensated for by a simultaneous decrease of the particle revolution frequency in the storage ring when the beam is inserted into the snake. In the case of complete insertion, the circumference change corresponds to the quantity $\Delta\Pi/\Pi \sim 10^{-4}$ ($\alpha \simeq 0.05$).

In fig. 3 is plotted a graph of the experimentally measured $\Delta\nu_x$ and $\Delta\nu_z$, in the case of beam insertion into the narrow part of the snake chamber without variation of the revolution frequency, with respect to the ratio of the magnetic field in one of the correction magnets and the maximum field value.

(3) Redistribution of the damping decrements G_x and G_s due to the fact that large orbital distortions arise in the four lenses of the straight section. If before the orbital distortion $G_x/G_z = 0.92$ and $G_s/G_z = 2.08$, then after it, these quantities are equal to: $G_x/G_z = 1.65$ and $G_s/G_z = 1.35$.

The orbit through the radius when inserting the beam was adjusted with the help of two radial plugs spaced in the direct vicinity of the snake and also by employing two pick-up stations to measure the position of the beam. A more precise adjustment was performed by visual observation of the light from the snake when operating with a weak magnetic field.

4. The influence of the snake field on the stored beam

The snake is composed of 18 magnets with alternating field sign which are connected in series. At the ends of the snake there are two more magnets but they have fewer ampere-turns. The latter are chosen in such a way that at maximum field in the basic magnets and in those at the edge the field is distinguished by a factor of two. However at small field levels when the iron core is not in the saturation regime, this relation is violated. As a result, when switching on the snake the beam orbit is changed. To compensate for this effect, a small corrector with vertical field is mounted on the one end of the snake. The current in this corrector is varied in proportion to the current in the snake winding before saturation of the iron cores. Moreover, the correction magnets H_2 and H_3 also participate in the compensation of the orbital variation.

When switching on the snake field an additional focusing appears [1] which is due to the focusing by the edge fields and also to the field inhomogeneity in the transverse horizontal direction. The behavior of $\Delta\nu_x$ and $\Delta\nu_z$ versus the current in the snake is shown in fig. 4. In the graph we can see the bend in the behavior of $\Delta\nu_z$ depending upon the current in the snake which is associated with saturation of the iron pole pieces.

In our case, the existence of a non-zero dispersion η-function at the location of the snake results in a significant limitation on the field value in the snake. This leads to a strong dependence of the damping decrements on the radial coordinate and, in addition, to a decreasing frequency range of revolution.

The damping decrements of radial betatron and synchrotron oscillations which are normalized over the decrement of vertical betatron oscillations may be derived from the expressions:

$$\frac{G_x}{G_z} = 1 - \frac{I_4}{I_2}; \qquad \frac{G_s}{G_z} = 2 + \frac{I_4}{I_2},$$

where

$$I_4 = \oint \left[\left(\frac{H}{H\rho} \right)^3 + \frac{2HG}{(H\rho)^2} \right] \eta \, ds ,$$

$I_2 = \oint [H^2/(H\rho)^2] \, ds$; H is the magnetic field, G the magnetic field gradient and $H\rho = (c/e)p$ (where p is the total momentum of the particles).

The snake magnetic field at the point shifted in the radial direction by the quantity $x = x_0$ and also in the vertical direction by the quantity $z = 0$ can be represented as follows:

$$H_x = 0 , \qquad H_s = 0 ,$$

$$H_z = H_0 \cos \frac{\pi x_0}{a} \sin \frac{\pi s}{b} ,$$

where a is the effective radial size of the snake, $2b$ the magnetic field variation period and H_0 the snake magnetic field amplitude.

In a first approximation the particle entering into the snake with the coordinate x_0 ($x_0/a \ll 1$) travels according to the law:

$$x = x_0 + \frac{H_0 b^2}{\pi^2 (H\rho)} \sin \frac{\pi s}{b} .$$

The additions to the integrals I_2 and I_4 which are due to the snake magnetic field may be estimated from the following expressions:

$$\Delta I_2 = \frac{H_0^2}{2(H\rho)^2} L_w ,$$

$$\Delta I_4 = - \frac{H_0^2}{(H\rho)^2} \left(\frac{\pi}{a} \right)^2 \eta L_w x_0 ,$$

where L_w is the snake length.

The integrals I_2 and I_4 (in the case when the snake field is off and with the correction magnets H_1, H_2, H_3, H_4 on) are equal, correspondingly, to:

$$I_2 = 0.00922 , \quad I_4 = -0.00599 .$$

Depending upon the value of the magnetic field H_0 and also the shift from the snake axis in the radial direction x_0, a relative damping decrement of radial betatron oscillations is written in the form:

$$\frac{G_x}{G_z} = 1 + \frac{0.00599 + (2100/\rho_0^2) x_0}{0.00922 + (45/\rho_0^2)} ,$$

where ρ_0 is the radius of curvature of the trajectory in the snake. This formula can be used for finding the range Δx, over which the damping of the radial betatron and synchrotron oscillations occurs simultaneously, i.e.

$$0 < G_x/G_z < 3 .$$

Whence, $\Delta x = 0.064 + 1.32 \times 10^{-5} \rho_0^2$.

It follows from the above formula that the range of variation of revolution frequency decreases with increasing snake field where damping of the synchrotron and betatron oscillations comes into play. This effect was noticed during operation of VEPP-3 and, in practice, this made it impossible to increase the snake field above 20 kG at an energy of 350 MeV.

A version of the VEPP-3 magnetic structure has been designed (not requiring technical improvements) with a zero dispersion function η at the location of the snake. This enables the damping decrement redistribution effect to be avoided in the case of the radial shift of the beam relative to the snake axis.

5. A study of undulator radiation

The question of electron radiation in the undulator magnetic field has been considered by various authors. That is why we will confine ourselves to simple considerations which illustrate the peculiarities of the spectral and angular distribution of the undulator radiation.

The electron which travels in the snake field radiates a pulse of electromagnetic waves in each magnet.

This wave pulse moves together with the electron and in a distance equal to the snake period the electron radiates a new pulse. At that moment, the preceding wave pulse passes the electron by a distance Δl due to, firstly, its higher velocity and, secondly, to the fact that in moving along the curved trajectory in the snake, the electron has to travel over a longer path. The retardation of the electron which passes through the snake period with respect to its light is expressed in the form:

$$\Delta l = 2b \left(\frac{1}{2\gamma^2} + \frac{\alpha_0^2}{4} + \frac{\theta^2}{2} \right) ,$$

where γ is the relativistic factor, $2b$ the snake period, $2\alpha_0$ the maximum bending angle of the electron orbit in each magnet of the snake and θ the angle with respect to the snake axis in the orbital plane at which the light is observed. After the transit of the electron through the snake periods the radiation field looks like a sign-variable alternation of the pulses with length $N\Delta l$ and period Δl.

If the width of one pulse $\sim \rho/\gamma^3$ is much less than

Δl, then the radiation spectrum differs slightly from the usual spectrum of synchrotron radiation.

In another limiting case, the length of the usual synchrotron radiation formation ρ/γ^3 is much larger than the snake period. For a weak magnetic field in the snake ($\alpha_0 \ll 1/\gamma$) the radiation field value is sinusoidal with a period Δl of length $N\Delta l$. Due to the finite length of the snake, the amplitude of the spectral constituent of the radiation with the wave number K is described by an apparatus function of the form:

$$E_K \sim \frac{K \sin(NK\,\Delta l/2)}{(2\pi/\Delta l)^2 - K^2}.$$

For the main maximum we can write down the following relation:

$$\lambda = 2b\left(\frac{1}{2\gamma^2} + \frac{\theta^2}{2}\right).$$

The latter gives a representation of the dependence between the correlation λ–θ and the energy. The form of the apparatus function makes it possible to determine the dependence of subsidiary maxima at a given K on the angle θ and on the energy as well. At the angle $\theta = 0$ in case of a weak field in the snake the radiation maximum is attained at the wavelength $\lambda = b/\gamma^2$. For the VEPP-3 snake this corresponds to a 920 Å vacuum ultraviolet region at an energy of 350 MeV.

The transverse motion becomes relativistic on increasing the snake field, and the shape of radiation field amplitude differs from the sinusoidal one, this leads to the appearance of harmonics in the radiation. The condition for the maximum of the nth harmonic can be written as follows:

$$n\lambda = 2b\left(\frac{1}{2\gamma^2} + \frac{\alpha_0^2}{4} + \frac{\theta^2}{2}\right).$$

An increase in α_0 results in increasing the wavelength of the first harmonic at zero angle. So, for example, the radiation of red light at this angle and for an energy of 350 MeV corresponds to a field of about 4 kG. For a snake with a finite number of periods N the above relation holds in a certain range of wavelengths $\Delta\lambda/\lambda = 1/nN$ at a fixed θ.

In fig. 5 there are the pictures of the intensity distribution of the 1st, 2nd, 3rd and 4th harmonics of radiation from the snake on a screen placed behind the red-light-filter at a fixed energy of 350 MeV and different values of the snake magnetic field.

The light from the snake passes through a special

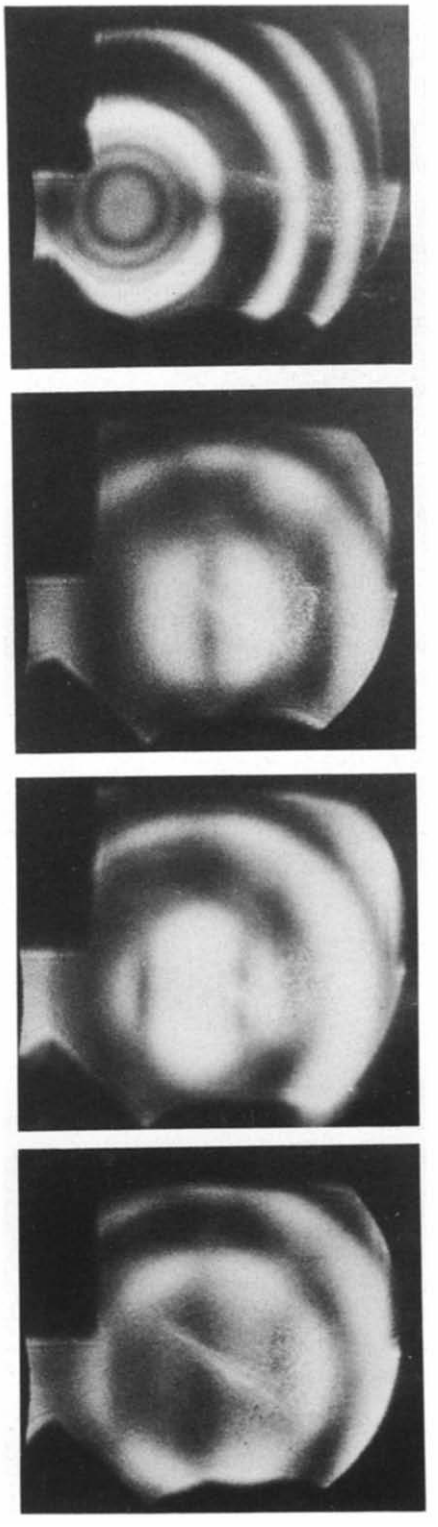

Fig. 5. Intensity distribution of the 1st, 2nd, 3rd and 4th harmonics of radiation from the snake.

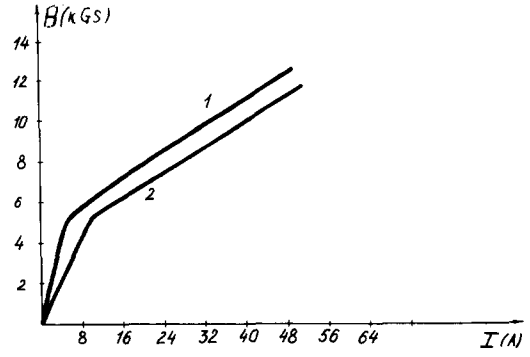

Fig. 6. Dependence of B on the current I in the snake.

vacuum channel sharing a common vacuum with the storage ring and through quartz glass of 80 mm diameter. This glass is situated at a distance of about 6 m from the center of the snake.

Observation of the red light at zero angle for different harmonics whose number is easily identified enables the behavior of the magnetic field in the snake to be determined, depending upon the winding current. For the VEPP-3 snake, when the red light is observed at zero angle, the magnetic field can be calculated using the formula:

$$B(KGs) = (19.4n - 2.75)^{1/2} ,$$

where n is the harmonic number.

The dependence of B on the current I in the snake is presented in fig. 6. Curve 1 corresponds to the measurement using the above described method. Curve 2 corresponds to the measurement of the betatron oscillation frequency shifts, dependent upon the current I.

In the graph the bend is clearly observed which corresponds to saturation of the snake iron cores.

The spectral composition of the radiation from the snake was analysed at zero angle with a spectrometer in the wavelength range from 2000–8000 Å. The design of the optics of the spectrometer is given in fig. 7.

The optics consist of an exit diaphragm 1, diffraction grating 2 with radius of curvature $R = 2$ m and number of lines $N = 600$ l/mm, and a controlled slit 3. This slit is placed so that the image of the source under study 0 is on its plane. As a receiver, the photomultiplier 4 is used, which operates in the regime of photon counting. The photomultiplier signal is amplified, transmitted to the recounting scheme, and then introduced to a computer. The scanning over the spectrum is performed by rotation of the diffraction grating 2 which is put in motion by a step-by step motor controlled with a computer. The motor step corresponds to a shift of the wavelength of $\Delta\lambda \simeq 54$ Å.

The radiation spectrum for the field $B = 6.8$ kG, which corresponds to the 3rd harmonic of the green light at zero angle, is drawn in fig. 8.

The peaks correspond to odd harmonics (even harmonics are suppressed at zero): the peak for the right edge corresponds to the 3rd harmonic of green light with wavelength of about 5500 Å, then the 5th harmonic with wavelength of about 3300 Å can be seen and on the left of it the seventh harmonic with wavelength 2350 Å. Then in the short-wave range a strong absorption of light occurs because of the non-transparency of the output glass and air in this wave range. There are also small peaks of even harmonics the presence of which may be explained by inaccurate adjust-

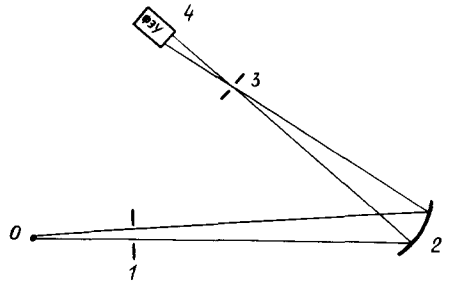

Fig. 7. Design of the optics of the spectrometer.

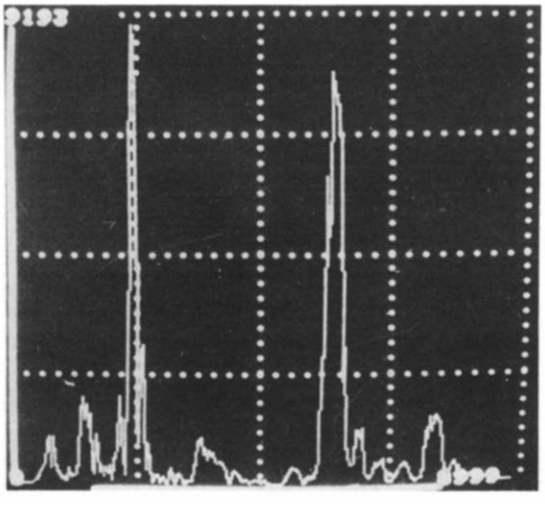

Fig. 8. Radiation spectrum for the field $B = 6.8$ kG.

ment at zero angle and the insufficiently small size of the exit aperture of the spectrometer. The width of these peaks corresponds to the widening due to the finite length of the undulator, i.e. $\Delta\lambda/\lambda = 1/nN$.

At the present, the snake and the correction magnets are under preparation for operation at an energy of 2.2 GeV. It is assumed that the maximum field at this energy will by available at the end of 1979.

References

[1] L.M. Barkov et al., Preprint INP 78-13, Novosibirsk (1978).
[2] L.M. Barkov et al., Nucl. Instr. and Meth. 152 (1978) 23.
[3] L.M. Barkov et al., Proc. of the 6th Natl. Conf. on Charged Particle Accelerators, vol. II, Dubna (1979) p. 267.
[4] D.F. Alferov et al., ZhETF, 42 (1972) 1921.